Analysis and optimization of fully foam-based capacitive sensors

Massimo Totaro, Irene Bernardeschi, Hongbo Wang*, Lucia Beccai
Center for Micro-BioRobotics, Istituto Italiano di Tecnologia (IIT), Pontedera, Italy
E-mails:massimo.totaro@iit.it, irene.bernardeschi@iit.it, hongbo.wang@iit.it, lucia.beccai@iit.it

***Abstract*— This paper presents the electromechanical analysis of ultra-light and highly compressible capacitive pressure sensors based on open-cell foams, with top and bottom surface electrodes built by PEDOT:PSS coating. Multiple samples of porous capacitive sensors were characterized, and experimental results were compared by means of both FEM simulations and theoretical analysis. The agreement between experiments and theoretical/numerical prediction is good, suggesting that this methodology can be a useful tool for fine tuning of the sensor performance (i.e. sensitivity, range) for specific applications. Finally, the proposed foam sensor provides a low-cost, easy-to-implement, robust sensing solution for real-world applications in robotics and wearable systems.**

Keywords— Soft sensors; conductive foam; capacitive pressure sensors; porous material modeling.

I. INTRODUCTION

Soft tactile sensors [1] are highly needed both in robotics [2],[3] and wearable systems [4], especially for mechanical interaction with environment and human motion monitoring. In the last decades, many transduction principles have been extensively investigated (resistive [5], capacitive [6], magnetic [7], inductive [8], optical [9],[10] etc.), with a particular effort in exploiting novel materials and smart structures [11]. Among main transducer mechanisms, capacitive sensors show the highest linearity and robustness to temperature and humidity variation. On the other hand, they need high sensitive read-out electronics, together with shielding solutions to electromagnetic noise and proximity effects [12].

In recent years, porous structures have attracted researchers in the field [13],[14],[15] for their intriguing characteristics. In particular, foams can experience very high compression strain without damaging, and they have been used as compressible materials for soft sensors. Due to this characteristic, foams are ideal candidate bulk material for building wearable devices, soft actuators and robots. Metal and carbon-based conductive nano-materials are commonly used as fillers for nanocomposites and as conductive coatings for foam-based sensors [16]. However, the conductivity is rather low and the bonding between the carbon nanomaterials and the polymer foam fibers is poor, a stabilization process is required to reduce the typical peeling-off effect. Recently, new type of resistive sensors based on highly conductive PEDOT:PSS and commercial polyurethane (PU) [17] and melamine [18] foam were developed.

Regarding capacitive sensors, one way to increase their sensitivity is to microstructure its surface, for exampling patterning pyramidal shapes or micro-nano pillars(cit) This mainly increases the effective sensor area, obtaining a larger output signal. Another very powerful approach is the introduction of micro-nanopores (ranging usually from 100 nm to 50 µm) in the dielectric layer. These have a double effect on the sensor performance. From the mechanical point of view, the stiffness of dielectric material can be finely tuned if micro-nano pores are used [19] and, applying the same pressure, a larger deformation is obtained with respect to a full structure, leading to a higher output signal. Moreover, the

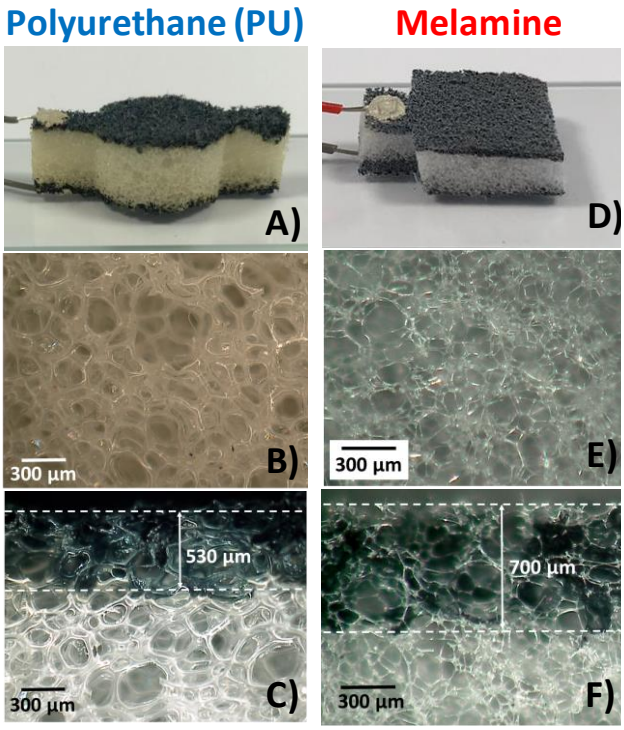

Fig 1.Polyurethane (PU) based capacitive sensor: Optical image of the whole device (A), of the open-cell foam (B), and cross section after PEDOT:PSS coating process (C), with a 530 µm thick conductive layer. Melamine based capacitive sensor: Optical image of the whole device (D), of the open-cell foam (E), and cross section after PEDOT:PSS coating process (F), with a 700 µm thick conductive layer.

*Hongbo Wang would like to thank the financial support of his Marie Skłodowska-Curie Individual Fellowship ("3D-SITS") from the European Union's Horizon 2020 research and innovation programme (No. 799773).

initial capacitance is lowered, due to the lower effective permittivity of the device, and this further increases the sensitivity. These effects can be further amplified by using foam structures as dielectric layer [20][21].

While several experimental works of foam based devices are present in the literature, their modeling is quite limited, due to the intrinsic high non linearity of these materials, and the difficulty to investigate their electrical behavior (i.e. the dielectric characteristics of such highly disordered porous structures).

In this work, we fabricated capacitive soft sensors with different dimensions, exploiting the high conductivity of poly(3,4-ethylenedioxythiophene) polystyrene sulfonate (PEDOT:PSS), and using two kind of commercial foams (PU and Melamine). Then, the experimental data were compared to numerical simulations, and used to validate a theoretical analysis on capacitive pressure sensors based on highly compressible foams. This methodology is useful for optimizing sensor performance (i.e. maximum signal output and pressure range) by tuning geometrical and physical (mechanical/electrical) properties of the device.

II. Foam Based Capacitive Sensor

A. *Fabrication process*

Cylindrical polyurethane (PU) foam samples with a radius of 8 mm were cut from a large commercial sheet (8643K549, McMaster-CARR, Chicago, USA) through a laser cutter, in order to make repeatable devices. Samples with different height were fabricated: 12 mm (PU-H1), 8 mm (PU-H2), and 4 mm (PU-H3). Also, square samples (with L=12 mm and H=4mm) were cut from a melamine resin foam large sheet (841006, Palustra, Levallois-Perret, France).

Capacitive sensors were fabricated by coating two opposite surfaces of foam samples with PEDOT:PSS as electrodes. The non-coated middle part of foam samples represent the dielectric of the capacitor. The PEDOT:PSS ink was prepared by mixing 95% PEDOT:PSS (Clevios PH1000, solid content 1.3%, Hereaus), 5% dimethyl sulfoxide (DMOSO, 99.9%, Sigma Aldrich), and 1% 4-dodecacylbenzenesulfonic acid (90%, Sigma-Aldrich). The electrodes (conductive surfaces) were obtained by dipping each surface in a small amount of ink corresponding to 1 µl/mm^2 for 30 seconds. The samples were then dried in a ventilated oven at 100° C for 20 minutes for each coated side. Finally, reliable contact with external wires were made by means of a stretchable silver conductor (PE873, DUPONT, Midland, USA).

Optical images of PU (A) and melamine (D) foam-based capacitive sensors samples are shown in Fig. 1, together with magnified open cell structures (Fig. 1B and 1E for PU and melamine, respectively). As described in a previous work [17], cells' size varies from 300 µm to 600 µm for PU foams, with a thickness of the fibers of ~50 µm. Melamine foam also showed cellular-like structure with cells size ranging from 100 to 250 µm, and fibers thickness ranging from 5 to 10 µm. In both cases, no morphological or structural differences could be noticed because of the heating process.

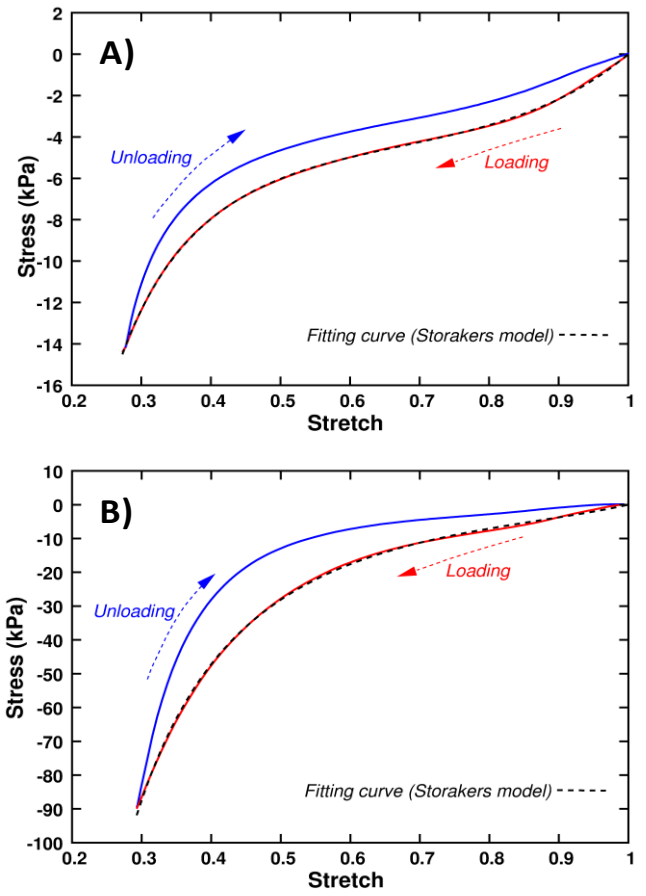

Fig. 2. Loading-Unloading stress-stretch experimental data with fitting curve using Storakers model (N=2) for FEM simulations for PU (A) and Melamine (B) foams, respectively.

Due to the above cell dimensions, the PEDOT:PSS ink film has a different morphology in the two foams. Indeed, in the case of PU, the ink coating resulted in the addition of a rough surface to the foam fibers with respect to the non-coated ones. Otherwise, in case of the melamine samples, the ink covered the fibers and it filled the hollow spaces between them, creating a suspended film. The thickness of conductive layers (t_{el}) was measured at optical microscope, observing an average value of 530 µm in the case of PU (Fig 1C), and around 700 µm for melamine (Fig. 1F). Finally, the sheet resistance resulted around 500 Ω/□ and 200 Ω/□ (corresponding around 2.5×10^{-2} Ω·m and 1.5×10^{-3} Ω·m) for the films on PU and melamine samples, respectively. Noticeably, the resistivity in the PU devices is around one order of magnitude greater than the one on melamine foam. This is because, in the latter case, the ink fills completely the cell pores, creating a continuous film.

B. *Experimental setup*

An experimental setup was built to characterize the mechanical and electrical behavior of the foam-based capacitive sensors. A cylindrical plastic indenter (15 mm diameter) was moved down to compress the top surface of the foam sensor samples controlled by a linear stage (M-111.1DG1, Physik Instrumente, Karlsruhe, Germany) with a

TABLE I. STORAKERS PARAMETERS FOR PU AND MELAMINE FOAMS

	μ_1 (kPa)	α_1	β_1	μ_2 (kPa)	α_2	β_2
PU	12.44	7.55	-0.15	3.87	7.79	-0.168
Melamine	18.3	12.12	0.063	5.64	-0.62	0.75e-3

step size of 10 µm at a speed of 0.3 mm/s. The applied pressure and capacitance were recorded on a PC through a commercial 6-axis load cell (Nano17, ATI Industrial Automation, Apex, USA) and a customized capacitance to digital converter (CDC) board, respectively, with a sampling frequency of 10 Hz. In Fig. 2 loading-unloading stretch-stress characteristics for PU (Fig.2A) and melamine (Fig.2B) foams are shown. In both cases, a strong non-linear behavior can be observed, as expected. Also, due to foam viscoelastic properties, hysteresis is well visible.

III. ELECTROMECHANICAL MODELING OF FOAM BASED CAPACITIVE SENSORS

A. Analytical model

From a mechanical point of view, the strong non-linear behavior of the foam must be taken into account. In this case, in order to reproduce the average mechanical behavior of a foam block, a second order (N=2) Storakers model [22] was implemented.

In particular, for uniaxial compression, the stretch (λ)-stress (σ) behavior can be expressed as

$$\sigma = \sum_{i=1}^{N} \frac{2\mu_i}{\alpha_i}\left(1-\lambda^{-\alpha_i\frac{1+3\beta_i}{1+2\beta_i}}\right)\lambda_i^{\alpha_i-1} \qquad (1)$$

Fitting parameters were extracted from the experimental stretch-stress curves acquired during experiments. Fitting curves for each foam are shown in Fig. 2 (dashed lines), and their corresponding parameters are reported in Table I. We can note that the melamine foam is stiffer than PU (stiffness is proportional, in first approximation, to µ parameters). This is also demonstrated by higher stretch-stress experimental curves.

From an electrical point of view, capacitance as a function of applied pressure P, can be expressed as

$$C(P) = \frac{k_0 A_0}{d_0}\frac{k_{eff}(P)}{1-\varepsilon(P)} \qquad (2)$$

where k_0, A_0, d_0 and $\varepsilon(P)$ are the vacuum dielectric constant, the device area, the dielectric initial thickness, and the strain (function of applied pressure), respectively. The $\varepsilon(P)$ function can be evaluated by inverting numerically Eq. (1), where $\lambda=1+\varepsilon$, for each pressure value. Due to its porous structure, the effective relative dielectric value heavily depends on pore shape, dimension and arrangement. Then, its behavior cannot be treated explicitly, and a custom equation, based on our previous work [19] can be introduced. In particular,

$$k_{eff} = k_{rp} - (k_{rp}-1)\frac{\phi_0}{1+{}^{P}/_{P_H}} \qquad (3)$$

where k_{rp} is the dielectric constant of the polymeric fiber, ϕ_0 is the initial porosity, P is the applied pressure, and P_H is a fitting parameter with the physical meaning of the pressure needed for halving initial porosity. k_{rp} was set to 3.5 and 10, and ϕ_0 is 0.96 and 0.99 for PU and melamine, respectively. Otherwise, P_H was fitted from experimental curves, as discussed in Section IV.

B. FEM simulations

In order to better analyze the electromechanical behavior of this kind of sensor and to further validate the analytical model, 2D-axisymmetric and 2D Finite Element Method (FEM) simulations were carried out, using commercial software COMSOL® Multiphysics v 5.4, for cylindrical and square devices, respectively. Usually, modelling foams is very challenging in FEM, due to their highly non-linear mechanical behavior, causing several convergence issues. In this case, in order to reproduce the average mechanical behavior of a foam block, second order Storakers model was implemented in COMSOL®, using parameters fitted from experiments, as shown in previous paragraph. This approach allowed stable mechanical simulations.

In order to validate the implemented model, FEM-calculated vertical displacement as a function of applied pressure was compared to its experimental counterpart. Results are shown in Fig. 3, where in solid and dashed lines experimental and FEM results are depicted, respectively.

From the electrical point of view, electrostatic simulations were performed, in order to calculate the device capacitance. Also in this case, the dielectric foam behavior cannot be simulated explicitly, and Eq. (3) was introduced for varying the effective relative dielectric constant upon external pressure. Finally, mechanics and electrostatics were coupled with moving mesh interface, in order to transfer mechanical deformations to the electrostatic study.

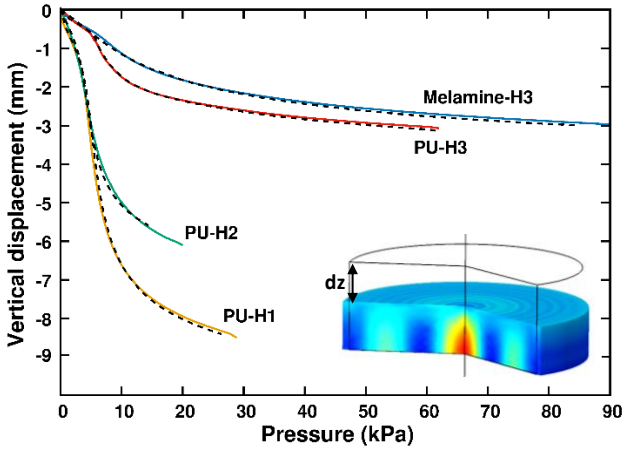

Fig. 3. Experimental vertical displacement (solid lines) versus applied pressure for different samples. FEM simulation results, using Storakers model, are shown with dashed line for each sample. In the inset, a sketch showing an example of the deformed structure computed by 2D axisymmetric FEM simulation.

IV. Results and Discussion

A. Output characteristics

All prototypes were tested with the setup described in Sec. II. In Fig. 4 experimental output characteristics (i.e. capacitance variation vs. applied pressure) of PU (Fig A-C) and Melamine (Fig 4D) foam based sensors are shown for loading and unloading (red solid lines). In all cases, hysteresis, due to foam viscoelasticity, is observable. Initial capacitance are of 1.5, 1.9, 2.4 and 4.65 pF for PU-H1, PU-H2, PU-H3 and melamine samples, respectively.

Experimental results are compared with FEM simulations (blue dashed lines) and analytical model (black dotted lines). In particular, for the latter, from Eq. (2) and (3), the capacitance variation can be written as

$$\Delta C(P) = \frac{k_0 A_0}{d_0}\left[k_{rp}\frac{\varepsilon(P)}{1-\varepsilon(P)} + \phi_0(k_{rp} - 1)\left(1 - \frac{1}{(1-\varepsilon(P))\left(1+{}^{P}/_{P_H}\right)}\right)\right] \quad (4)$$

where $\varepsilon(P)$ can be calculated numerically by inverting Eq. (1). In addition, P_H = 1 MPa for PU, and P_H = 3 MPa for melamine gave the best fitting of Eq. (4) with experimental curves (shown in Fig. 4). This is consistent with the fact that melamine foam is stiffer than PU, needing a higher pressure to halve its initial porosity.

In all cases, both FEM and analytical curves agree well with experimental data. Also, it must be noted that both numerical and analytical analysis are made for quasi-static conditions. Thus, they do not include any dynamic effect (i.e. viscoelasticity, etc), and they are reliable only for loading curves.

Regarding sensitivity, two main regions can be identified from the output curves. Indeed, for very low pressure, the capacitance variation (and consequently device sensitivity) results quite low, while it has a significant increase after a particular pressure value. This is a direct consequence of foam mechanical behavior, where a stiffer elastic-like and a softer viscoelastic regime can be revealed. In particular, for PU samples, sensitivities of around 8×10^{-3} kPa^{-1} up to 3.5 kPa (PU-H1), 10^{-2} kPa^{-1} up to 4 kPa (PU-H2), and 2×10^{-2} kPa^{-1} up to 5.5 kPa (PU-H3) are retrieved. It can be observed that the pressure limit for this range increases with the height of the sample, but with a decreasing sensitivity. Oppositely, this first linear regime cannot be revealed in the melamine foam, being consistent to its mechanical characteristics. Otherwise, higher sensitivities in the viscoelastic region are measured: around 4.2×10^{-2} kPa^{-1} (PU-H1), 5×10^{-2} kPa^{-1} (PU-H2), 4.3×10^{-2} kPa^{-1} (PU-H3) and 1.6×10^{-2} kPa^{-1} (Melamine). In this case, no clear dependence on different height and material can be observed, since all values are in the same range.

Finally, signal stability was investigated by long term loading-unloading cycles. As example, 100 cycles for PU-H2 device are shown in Fig. 5A, where an average drift of -50 fF/min can be measured.

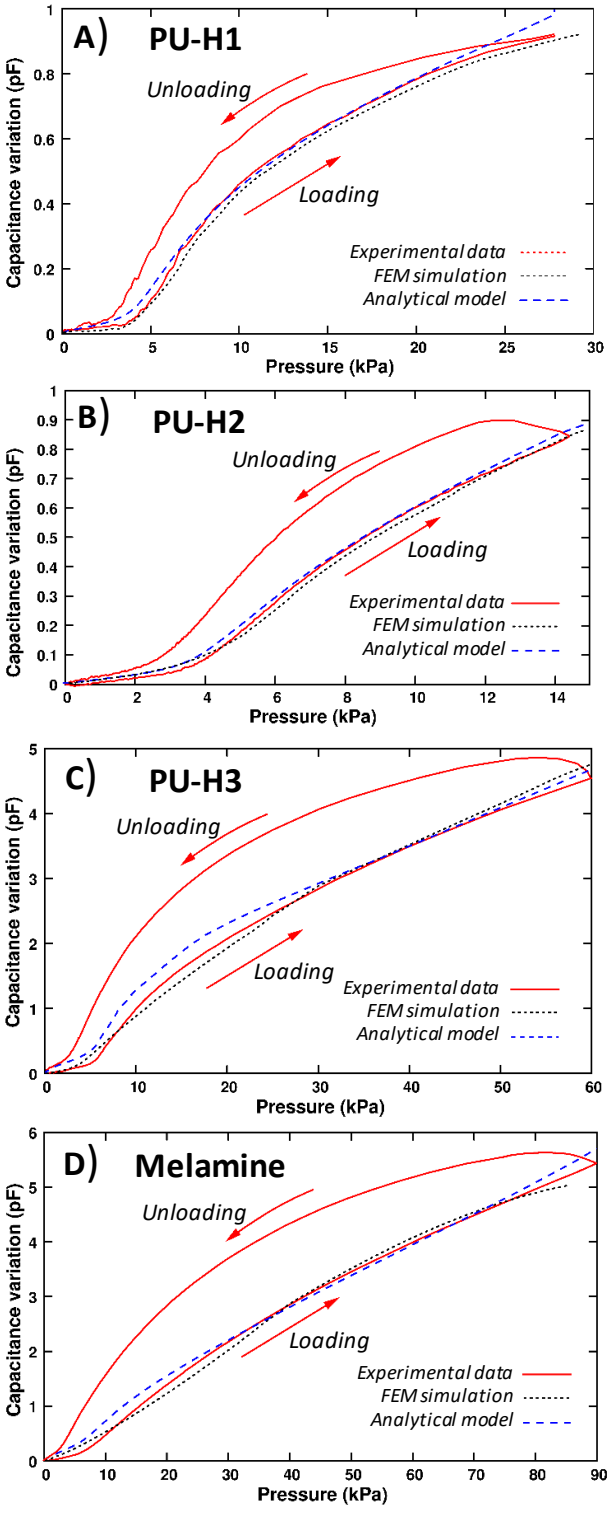

Fig. 4. Outuput characteristics (red solid lines) for PU-H1 (A), PU-H2 (B), PU-H3 (C), and Melamine (D) samples, compared with corresponding FEM simulation (black dotted lines) and analytical prediction (blue dashed lines).

C. *Maximum pressure range and sensor optimization*

A key aspect to be considered in this kind of sensor is the maximum pressure range that they can sustain. Since the compression reduces the electrode distance, they will come in contact at a certain pressure value, avoiding further capacitance measurement. In first approximation, uniform strain is assumed for the whole device. Hence, the maximum achievable strain is $\varepsilon_{MAX} = (H-2t_{el}\cdot\varepsilon_{MAX})/H$, so that $\varepsilon_{MAX} = H/(H+2t_{el})$, where H is the device height and t_{el} the electrode thickness. In the case of tested device, maximum strain is around 92%, 88%, 80% and 73% for PU-H1, PU-H2, PU-H3 and melamine, respectively. Then, maximum pressure P_{MAX} can be calculated from Eq. (1), finding around 130 kPa, 100 kPa, 70 kPa and 120 kPa, respectively. Finally, using these values in Eq. (4), the maximum capacitance variation can be retrieved. For tested samples, it results around 2.5 pF, 3.7 pF, 8 pF, and 6.5 pF, respectively. More in general, the electro-mechanical behavior of this kind of devices can be evaluated with the system of Eq. (1) and (4). In this way, several parameters can be tuned in order to optimize the sensor performance for a specific application, maximizing either the sensor output variation (and, consequently, its sensitivity) or the maximum pressure range.

In Fig. 5B the theoretical behavior (in dashed line) of the maximum capacitance variation vs. maximum pressure range is shown for k_{rp} = 3.5 (PU foam) and k_{rp} =10 (Melamine foam). Also, solid markers show the values for devices tested experimentally. As general trend, capacitance variation increases with krp and decreases with d_0. Thinner sensors can give a higher signal output, but, on the other hand, lower maximum pressure can be reached. In addition, also foam stiffness plays a role in this behavior, since stiffer materials can provide higher maximum pressure range but, at the same time, lower maximum capacitance variation. Then, a trade-off between maximum signal output and maximum pressure range is needed.

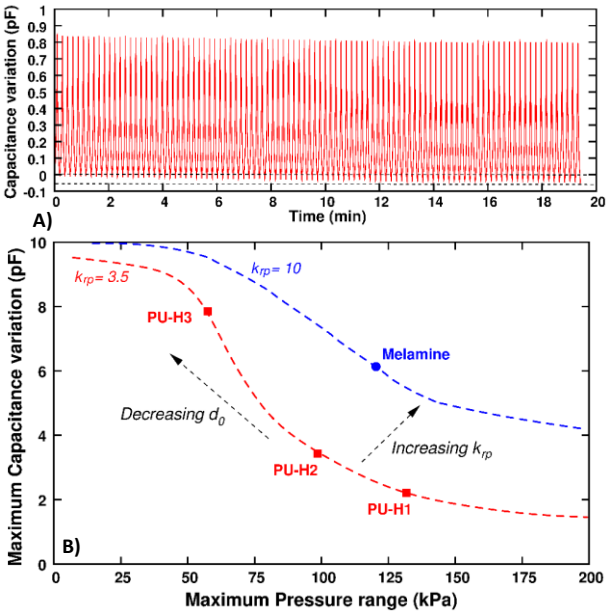

Fig. 5. A) Long-term stability and repeatability test over 100 loading-unloading cycles, showing an average drift of about -50 fF/min. B) Behavior estimation of the maximum capacitance variation vs. the maximum pressure range, based on the theoretical analysis, varying sensor height (d_0) and polymer dielectric constant (k_{rp}). Solid marks show values for tested devices.

The analysis above allow us to predict the sensor performance according to its geometry and to mechanical/electrical properties, enlightening which parameters can be tuned for optimal performance in a specific application. For instance, if a particular pressure range is known, sensor performance can be maximized by tuning all other parameters. On the contrary, if a particular signal variation is sufficient for some scenarios (i.e. control loop in a soft robot), the pressure range can be maximized for given geometrical constraints and material options.

V. CONCLUSIONS

In summary, we presented a novel methodology to optimize the performance of low-cost, ultra-light, and highly compressible capacitive pressure sensors based on different commercial foams, and coated with PEDOT:PSS at top and bottom surface for building electrodes. In particular, for the mechanical behavior, 2nd order Storakers model was adopted, and exploited for both analytical model and FEM simulations. From an electrical point of view, a custom equation was introduced in order to include the effect of porosity in the effective relative permittivity, which varies with applied pressure.

From an experimental point of view, samples with different geometries and mechanical/electrical properties were fabricated and tested. Both FEM simulations and analytical results agree well with experimental data. Then, this method provides a tool for optimizing the performance of soft capacitive sensors fully based on foam materials. In general, there is a trade-off between the maximum pressure range and the maximum sensor output signalm and geometry and mechanical/electrical properties can be varied in order to balance these ranges.

In next future, a more extensive analysis can be performed, including different shapes, dimensions and types of foams (both commercial and custom-made). This low-cost and versatile sensing solution looks very promising for 3D multimodal sensing in wearable systems, soft robots and actuators (*i.e.* pneumatic artificial muscles). Indeed, sensory foams can provide useful information (on both proprioception and exteroception) without introducing undesired additional stiffness and then affecting the mechanical characteristics of the soft system.

REFERENCES

[1] M. R. Cutkosky, R. D. Howe, and W. R. Provancher, "Force and tactile sensors," in Springer Handbook of Robotics: Springer, 2008, pp. 455-476.

[2] H. Wang, M. Totaro, and L. Beccai, "Toward perceptive soft robots: Progress and challenges," Advanced Science, vol. 5, no. 9, p. 1800541, 2018.

[3] P. S. Girão, P. M. P. Ramos, O. Postolache, and J. M. D. Pereira, "Tactile sensors for robotic applications," Measurement, vol. 46, no. 3, pp. 1257-1271, 2013.

[4] G. Ge, W. Huang, J. Shao, and X. Dong, "Recent progress of flexible and wearable strain sensors for human-motion monitoring," Journal of Semiconductors, vol. 39, no. 1, p. 011012, 2018.

[5] S. Stassi, V. Cauda, G. Canavese, and C. F. Pirri, "Flexible tactile sensing based on piezoresistive composites: A review," Sensors, vol. 14, no. 3, pp. 5296-5332, 2014.

[6] L. Viry et al., "Flexible three-axial force sensor for soft and highly sensitive artificial touch," Advanced Materials, vol. 26, no. 17, pp. 2659-2664, 2014.

[7] H. Wang et al., "Design Methodology for Magnetic Field-Based Soft Tri-Axis Tactile Sensors," Sensors, vol. 16, no. 9, p. 1356, 2016.

[8] H. Wang et al., "Robust and High-Performance Soft Inductive Tactile Sensors based on the Eddy-Current Effect," Sensors and Actuators A: Physical, 2017.

[9] M. Ramuz, B. C. K. Tee, J. B. H. Tok, and Z. Bao, "Transparent, optical, pressure-sensitive artificial skin for large-area stretchable electronics," Advanced Materials, vol. 24, no. 24, pp. 3223-3227, 2012.

[10] M. Totaro, A. Mondini, A. Bellacicca, P. Milani, and L. Beccai, "Integrated simultaneous detection of tactile and bending cues for soft robotics," Soft robotics, 4(4), 400-410, 2017.

[11] T. Yang, D. Xie, Z. Li, and H. Zhu, "Recent advances in wearable tactile sensors: Materials, sensing mechanisms, and device performance," Materials Science and Engineering: R: Reports, vol. 115, pp. 1-37, 2017.

[12] M. Totaro et al., "Soft smart garments for lower limb joint position analysis", Sensors, 17 (10), 2314, 2017.

[13] H. Ding et al., "Influence of the pore size on the sensitivity of flexible and wearable pressure sensors based on porous Ecoflex dielectric layers", Materials Research Express, 2019.

[14] Y. Ding, T. Xu, O. Onyilagha, H. Fong, and Z. Zhu, "Recent Advances in Flexible and Wearable Pressure Sensors Based on Piezoresistive 3D Monolithic Conductive Sponges," ACS Applied Materials & Interfaces, 2019.

[15] J. Qiu et al., "Rapid-Response, Low Detection Limit, and High-Sensitivity Capacitive Flexible Tactile Sensor Based on Three-Dimensional Porous Dielectric Layer for Wearable Electronic Skin," ACS Applied Materials & Interfaces, vol. 11 no. 43, pp. 40716-40725, 2019.

[16] X. Wu, Y. Han, X. Zhang, Z. Zhou, and C. Lu, "Large-area compliant, low-cost, and versatile pressure-sensing platform based on microcrack-designed carbon Black@ polyurethane sponge for human–machine interfacing," Advanced Functional Materials, vol. 26, no. 34, pp. 6246-6256, 2016.

[17] H. Wang, I. Bernardeschi, L. Beccai, "Developing Reliable Foam Sensors with Novel Electrodes", Proc. of the IEEE Conference on Sensors, 27-30 October, 2019. Montreal, Canada (*in press*).

[18] Y. Ding, J. Yang, C. R. Tolle, and Z. Zhu, "Flexible and Compressible PEDOT:PSS@Melamine Conductive Sponge Prepared via One-Step Dip Coating as Piezoresistive Pressure Sensor for Human Motion Detection," ACS Appl Mater Interfaces, vol. 10, no. 18, pp. 16077-16086, 2018.

[19] M. Totaro, and L. Beccai, "Electromechanical behavior of soft porous capacitive sensors", Proc. of the 1st IEEE International Conference on Soft Robotics (RoboSoft), pp. 233-238, April 2018.

[20] J. Qiu et al., "Rapid-Response, Low Detection Limit, and High-Sensitivity Capacitive Flexible Tactile Sensor Based on Three-Dimensional Porous Dielectric Layer for Wearable Electronic Skin," ACS Applied Materials & Interfaces, vol. 11 no. 43, pp. 40716-40725, 2019.

[21] C. Parameswaran and D. Gupta, "Low cost sponge based piezocapacitive sensors using a single step leavening agent mediated autolysis process," Journal of Materials Chemistry C, vol. 6, no. 20, pp. 5473-5481, 2018.

[22] Ju, Ming Lei, et al. "Parameter estimation of a hyperelastic constitutive model for the description of polyurethane foam in large deformation." Cellular Polymers vol. 32 no. 1, pp. 21-40, 2013